



UDC 621.7

## SIMULATION OF BORING BY SMOOTHED PARTICLE HYDRODYNAMICS METHOD

Maksym Shykhaliyev

*National Technical University of Ukraine «Igor Sikorsky Kyiv Polytechnic  
Institute», Kyiv, Ukraine*

**Summary.** The possibility of applying the smoothed particle hydrodynamics method for modeling of cutting processes on the example of multi-blade boring of holes is considered in this paper. Highly nonlinear LS-Dyna solver with an explicit statement of the dynamic modeling problem is used as a software package for modeling. Johnson-Cook formulation with the corresponding empirical coefficients for each material is used as the model of the workpiece material. Absolutely solid tool is used to simplify the model. The kinematic scheme of the tool rotation is implemented using the keyword INITIAL\_VELOCITY\_GENERATION. The simulation results obtained in the software package are presented in the form of graphs.

**Key words:** boring, cutting dynamics, smoothed particle hydrodynamics method, mesh-free modeling method, FEM, SPH, machining modeling.

[https://doi.org/10.33108/visnyk\\_tntu2021.03.013](https://doi.org/10.33108/visnyk_tntu2021.03.013)

Received 01.09.2020

**Introduction.** Smoothed particle hydrodynamics (SPH) method is a mesh-free promising alternative to well-known grid-based simulation methods, such as the finite element method (FEM), in the investigation of metalworking processes characterized by highly dynamic behavior and large deformations relatively to initial configuration. This method, among the others, can take into account the thermal aspects of machining. Also, this method does not require adaptive remeshing, during which the calculation accuracy can be lost. And the continuum is discretized by the cloud of numerical integration points [1]. These points, called particles, are the basis of the kernel functions required for differential equations integration. The disadvantages of this method include the lack of version for implicit problems (implicit dynamics) solution in the software package LS-Dyna [14] and the geometric inaccuracy of the obtained chips during machining [1]. Modeling by smoothed particle hydrodynamics method is shown on the example of multi-blade boring of parts made of various materials taking into account thermal effects. The application specifications for different materials with the corresponding parameters of the material model are investigated. The largest integration step for convergence in numerical solution of the machining problem is limited by Courant-Friedrichs-Levy criterion [2].

The development of computer methods for machining processes modeling made it possible to optimize machining parameters using natural experiments as tests, which greatly simplified the scientific researches. Analysis of scientific publications revealed the absence of boring process modeling by smoothed particle method taking into account the kinematic machining scheme as all cutting process investigations by means of LS-Dyna solver are reduced to simple orthogonal cutting modeling that does not take into account dynamic boring processes.

**Literature review.** The smoothed particle hydrodynamics method is increasingly used by scientists in the development of computer models of cutting process [9, 10, 3]. For example, the model of turning orthogonal processing of INCONEL 718 material at cutting speed

100 m/min, presented by researchers [9], has an error in the cutting forces investigation not greater than 9% compared to the carried out experiments. Madaj and Piska [3] presented the model of orthogonal turning using smoothed particle hydrodynamics method for aluminum alloy A2024-T351 with cutting speed up to 800 m/min. Moreover, the modeling error in cutting forces investigation by SPH and mesh (FEM) method is not greater than 10%. C45E grade steel milling is presented in the investigation [1]. The graph of experimental and simulated cutting force for non-orthogonal cutting is given. Simulation of stone fracture under the action of disk cutter of tunneling-boring machine was carried out in the investigation [16] using the finite element method. The distribution of forces during cutting in dynamics is shown. The process of microcutting is studied in paper [17]. The investigation of the regenerative oscillations occurrence during turning is carried out in paper [18]. SPH method is used to develop machining models with additional heat treatment of Ti6Al4V in the investigation [13]. The model of orthogonal cutting of AISI 1045 steel is investigated in paper [10]. However, boring process using smoothed particles is not studied, the simulation is performed by classical mesh method.

**Objective of the investigation.** Development of computer model of boring holes in different materials using LS-Dyna solver by smoothed particle method in order to determine the cutting forces.

**Statement of the problem.** Creation of computer boring model with appropriate kinematic scheme of machining by smoothed particle method using LS-Dyna solver.

**Description of the computer model.** In order to create numerical processing model, it is proposed to use the mesh-free modeling method. The ratio of stresses and strains can be described by means of Johnson-Cook material model. This relationship is described by the following equation 1 [2].

$$\sigma_v = (A + B \cdot p^r) \left[ 1 - \left( \frac{T - T_r}{T_m - T_r} \right)^m \right] \left( 1 + C \cdot \ln \left( \frac{\dot{p}}{\dot{\varepsilon}_0} \right) \right) \quad (1)$$

where  $\sigma_v$  is equivalent stress in the material,  $p$  is equivalent plastic deformation,  $T$  is temperature parameter for the given material,  $T_r$  is environment temperature (room),  $T_m$  is melting temperature for the given material,  $\dot{\varepsilon}_0$  is reference strain rate. Coefficients  $A$ ,  $B$ ,  $C$ ,  $r$ ,  $m$  are parameters of the given material for Johnson-Cook model.

It is important to describe the mechanism of workpiece material fracture. To model this mechanism, it is necessary to use the material fracture criterion (for Johnson-Cook material model). According to this criterion, the equivalent voltage  $\sigma_v$  is sharply set to zero during its performance. The fracture function  $e_f$  depends on the fracture parameters of material D1-5 and  $e_{f \min}$ . The criterion of physical fracture in the material model is given by equation 2 [1].

$$e_f = \max \left\{ \left[ D_1 + D_2 \exp \left( D_3 \cdot \frac{p}{\sigma_{eff}} \right) \right] \left[ 1 + D_4 \ln \frac{\dot{p}}{\dot{\varepsilon}_0} \right] \left[ 1 + D_5 \frac{T - T_r}{T_m - T_r} \right], e_{f \min} \right\} \quad (2)$$

where  $D_1$ ,  $D_2$ ,  $D_3$ ,  $D_4$ ,  $D_5$  – are empirical coefficients set for each material grade and can be found in scientific literature [1, 2, 14],  $p$  is equivalent plastic deformation,  $\sigma_{eff}$  is effective stress,  $\dot{p}$  is indicator of plastic equivalent deformation, control strain rate,  $e_{f \min}$  – lower limit of fracture deformation,  $T$  – temperature parameter for the given material,  $T_r$  is environment temperature (room),  $T_m$  is melting point for the given material.

Thus, the equivalent stress in material model depends on the temperature, the rate of equivalent plastic deformation, the coefficient of equivalent plastic deformation.

For modeling the cutting processes in LS-Dyna software package, the relevant material parameters as well as mechanical characteristics of the materials are input into the keyword

card of LS-Dyna solver. Their numerical values for each material are summarized in Table 1, 2, and also 3 (given below).

The numerical computer model is developed in the software package of highly non-linear LS-Dyna solver, the workpiece is generated by smoothed particle hydrodynamics method, and the tool – by mesh. The influence of thermomechanical behavior on cutting forces is significant [11], so it is recommended to use Johnson-Cook material model [12], which takes into account thermal effects during machining, or other models for thermomechanical problems.

The tool movements during simulation are specified by means of the solver key words \* INITIAL\_VELOCITY\_GENERATION for rotational movement of the tool (300 rad/s or about 48 rot/s) and \* BOUNDARY\_PRESCRIBED\_MOTION to specify the tool translational movement. The workpiece is fixed by the boundary conditions of the system freedom degrees. The parameters of high-speed cutting in the model are given due to the cutting speed  $V_c = 300$  m/min and are assumed to be the same for all materials. The environment temperature  $T_r$  is taken as  $24^\circ\text{C}$ . The workpiece hole diameter is 224 mm, the workpiece length is 330 mm. The cut layer width is the same for each material and is equal to 5 mm. The cutting thickness is 3 mm. The cutting depth is 5 mm. The mandrel diameter is 150 mm. The material of the cutting part is C45E steel. The number of boring cutters is 3. The front angle is  $15^\circ$ , the main angle in the plan is  $30^\circ$ , the auxiliary angle in the plan is  $15^\circ$ .

The parameters of material model for heat-resistant nickel-chromium alloy Inconel 718 [1], steel C45E [2], aluminum alloy A2024-T351 [3] are given in Table 1. Johnson-Cook material model is used for the workpiece. This model is empirical and makes it possible to take into account changes in temperature and strength, kinematic and isotropic hardening. The Rigid type is chosen for the tool material model, which is absolutely solid. High-speed steel is accepted as the cutting part material. Accordingly, the tool is made in the classic form of elements mesh. The steel density for the tool model is  $7800\text{ kg/m}^3$ . Coolants are not taken into account in the simulation. Table 2 shows the coefficients for models of Johnson-Cook materials [1, 2, 3]. The mechanical characteristics of materials used in keywords MAT\_JOHNSON\_COOK, MAT\_THERMAL\_ISOTROPIC solver are shown in Table 3.

**Table 1**

Parameters of Johnson-Cook material model for the solver

		Material model parameters							
		A, MPa	B, MPa	C	r	m	$T_m, ^\circ\text{C}$	$T_r, ^\circ\text{C}$	$\varepsilon_0$
Material	Inconel 718	450	1700	0.017	0.65	1.3	1297	28	0.001
	Steel C45E	553	600	0.0134	0.234	1	1480	28	0.001
	A2024-T351	352	440	0.42	0.09	1.03	1520	28	0.001

**Table 2**

Johnson-Cook material model coefficients for the solver

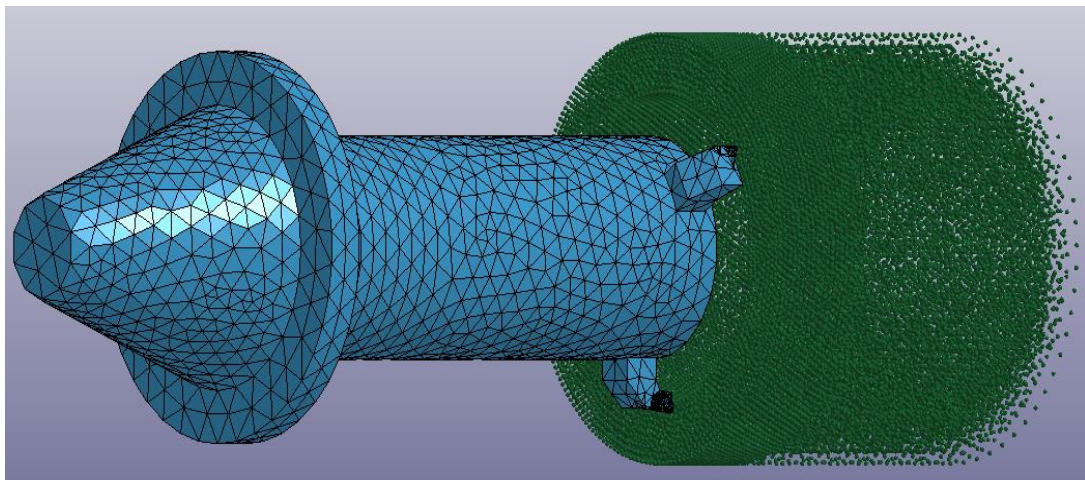
		Material model parameters					
		D1	D2	D3	D4	D5	$\varepsilon_{fmin}$
Material	Inconel 718	0.11	0.75	-1.45	0.04	0.89	0
	C45E	0.06	3.31	-1.96	0.0018	0.58	0
	A2024-T351	0.13	0.13	-1.5	0.011	0	0

**Table 3**

Mechanical characteristics of materials used in the model

Material	Mechanical characteristics
Inconel 718	Density $\rho$ , $8.22 \cdot 10^3 \text{ kg/m}^3$ Young's modulus $E$ , $2.8 \cdot 10^{11} \text{ N/m}^2$ Poisson ratio $\nu$ , 0.3 Liquidity limit $\sigma_y$ , $8.2 \cdot 10^8 \text{ N/m}^2$ Strain fracture $\epsilon_f$ , Specific heat at constant pressure $c_p$ , $680 \text{ J/(kg} \cdot ^\circ\text{C)}$ Thermal conductivity $\lambda$ , $11.4 \text{ W/(m} \cdot \text{K)}$
C45E	Density $\rho$ , $7.80 \cdot 10^3 \text{ kg/m}^3$ Young's modulus $E$ , $2.10 \cdot 10^{11} \text{ N/m}^2$ Poisson ratio $\nu$ , 0.3 Liquidity limit $\sigma_y$ , $5.53 \cdot 10^8 \text{ N/m}^2$ Strain fracture $\epsilon_f$ , $1.33 \cdot 10^{-1}$ Specific heat at constant pressure $c_p$ , $460 \text{ J/(kg} \cdot ^\circ\text{C)}$ Thermal conductivity $\lambda$ , $55 \text{ W/(m} \cdot \text{K)}$
A2024-T351	Density $\rho$ , $2.7 \cdot 10^3 \text{ kg/m}^3$ Young's modulus $E$ , $2.7 \cdot 10^{11} \text{ N/m}^2$ Poisson ratio $\nu$ , 0.3 Liquidity limit $\sigma_y$ , $280 \text{ MPa}$ Specific heat at constant pressure $c_p$ , $875 \text{ J/(kg} \cdot ^\circ\text{C)}$ Thermal conductivity $\lambda$ , $121 \text{ W/(m} \cdot \text{K)}$

In fig. 1 shows The screenshot of the model for boring investigation in solver LS-Dyna is presented in Fig. 1.

**Figure 1.** Computer model of boring with tool mesh and workpiece

The highly non-linear LS-Dyna solver makes it possible to choose a wide range of criteria for removing the workpiece material according to the solver keywords that can be found in the literature, particularly in LS-Dyna Keyword Manual [15].

In order to solve the simulation problem, we use personal computer with LS-Dyna SMP setting (shared memory parallel processing), processor with two cores and clock speed 3.3 GHz, 4 GB of RAM. The calculation time is 5.5 hours.

**The results of the investigation.** Graphs are constructed by means of internal tools and LS-Dyna solver interpreter. Graphs of the change in equivalent Mises stresses over time at the cutting area for each of the materials (a-c) are shown in Fig. 2. It is evident from Fig. 2 a, that the value of equivalent stresses during hole boring made of heat-resistant Inconel 718 grade alloy (analog according to ISO 6208 standard) is relatively constant and fluctuates around the value of 522 GPa. For materials of steel and aluminum alloy, the values of equivalent stresses according to Mises have more apparent significant fluctuations. The sharp peak stress for C45E grade steel (analog Steel 45) is approximately 800 GPa at the beginning and gradually decreases as shown in Fig. 2 b. The peak sharp value for aluminum alloy A2024-T351 (analog D16T) is 410 GPa (Fig. 2 c), respectively. It is achieved by cutting the cutting tool into the workpiece and then decreases. Figure 3–5 shows the graph of the cutting force. As it is evident from the cutting forces graphs, the fluctuations of the cutting force during boring in the given model has the largest amplitude for A2024-T351 grade aluminum alloy. For other two materials, the fluctuations of the cutting forces have smaller amplitude and peak value of the cutting force. Relatively, the smallest fluctuation of cutting forces is obtained for C45E steel.

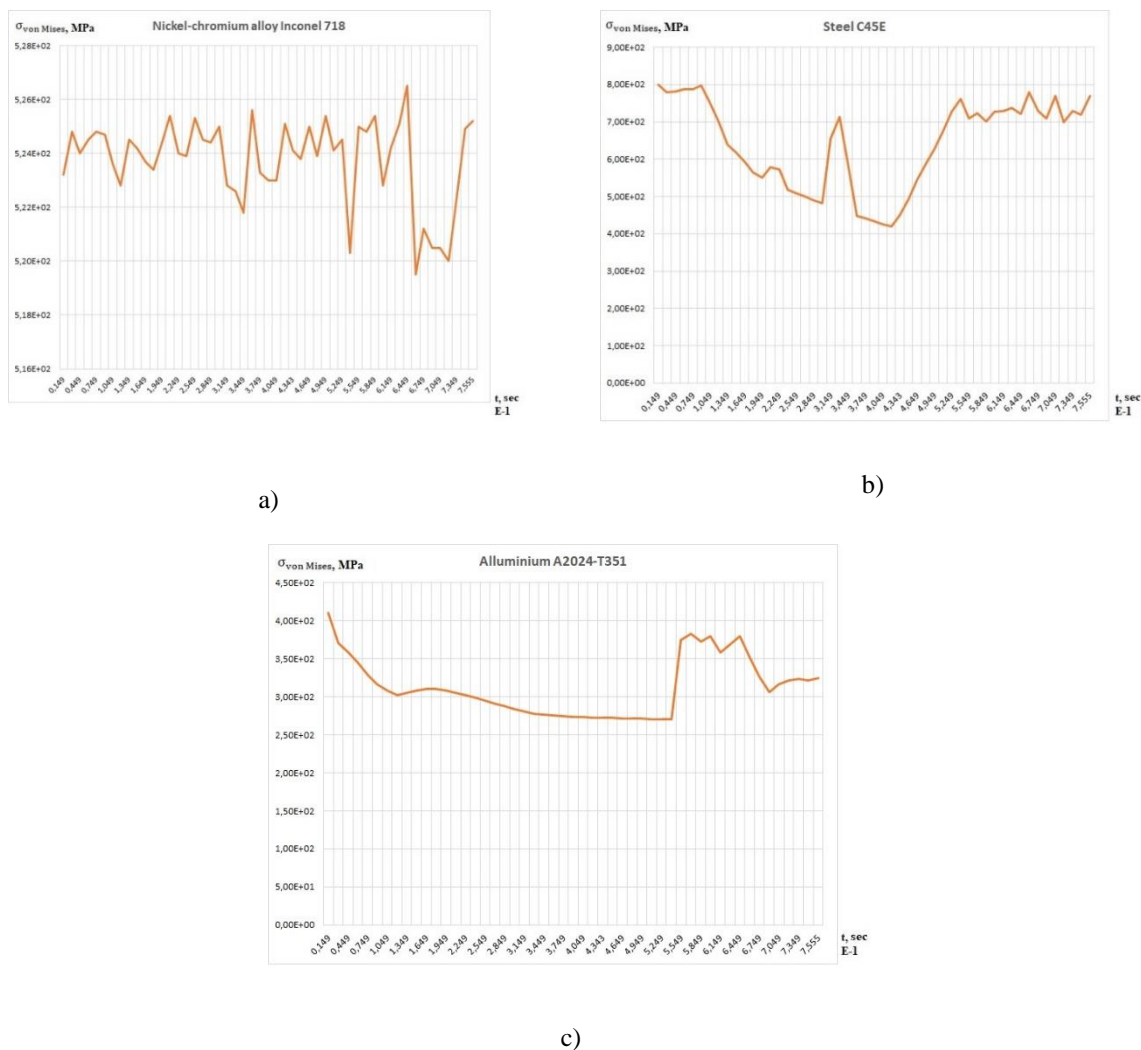


**Figure 2.** Changes in equivalent stresses by Mises in time at the cutting area for each material:  
a) for Inconel 718, b) for C45E grade steel, c) for A2024-T351 grade aluminum

The effective plastic deformation  $\varepsilon_p$  is used as erosion criterion to remove damaged elements in numerical simulation. It is an accumulative quantity and its value is defined as the integral of plastic deformations increase over a certain period of time. The effective plastic deformation increases when the material is actively deformed, i.e. when the stress is at the yield point on the contact surface of the tool-workpiece. The graphs of changes in the effective plastic deformation  $\varepsilon_p$  for each material are represented in Fig. 6–7. In Fig. 6 graph 1 corresponds to Inconel 718 material, graph 2 corresponds to steel C45E material.

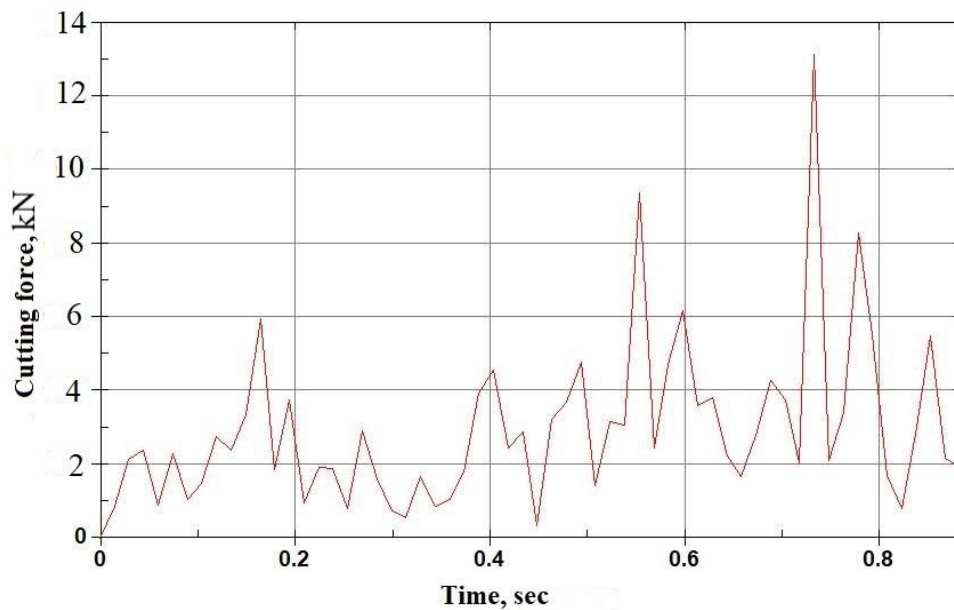


**Figure 3.** Cutting force in the simulation of boring for Inconel 718 material

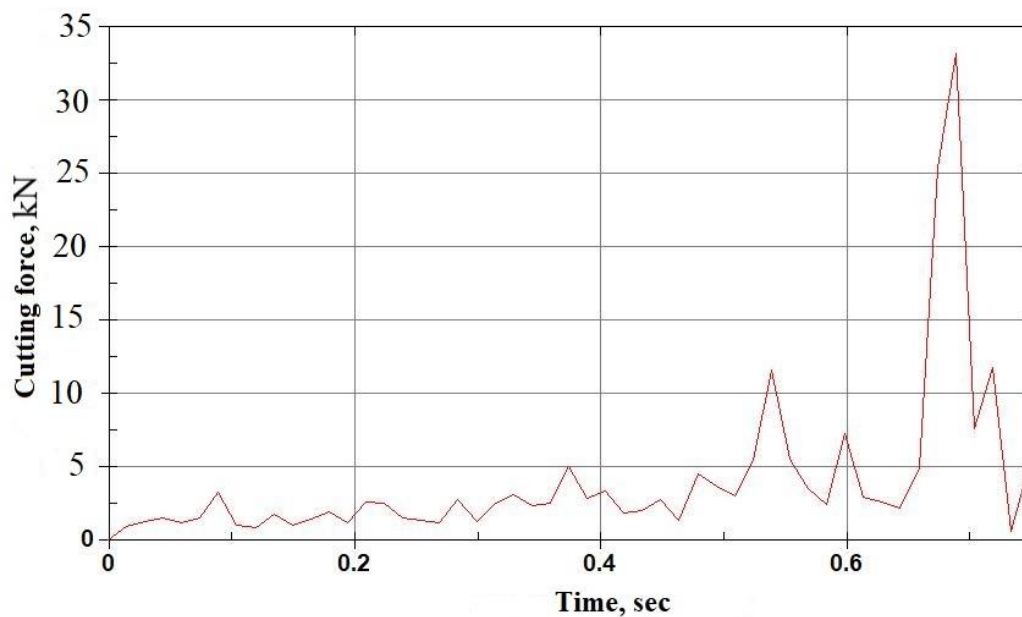


**Figure 4.** Cutting force in the simulation of boring for steel C45E material

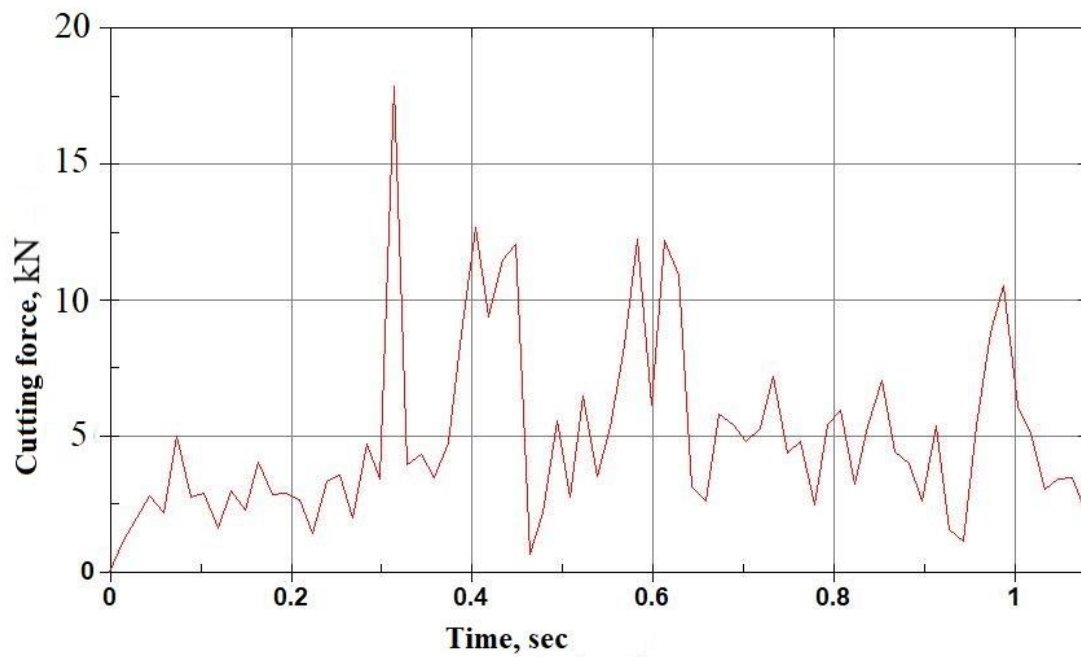


**Figure 5.** Cutting force in the simulation of boring for A2024-T351 grade aluminum material

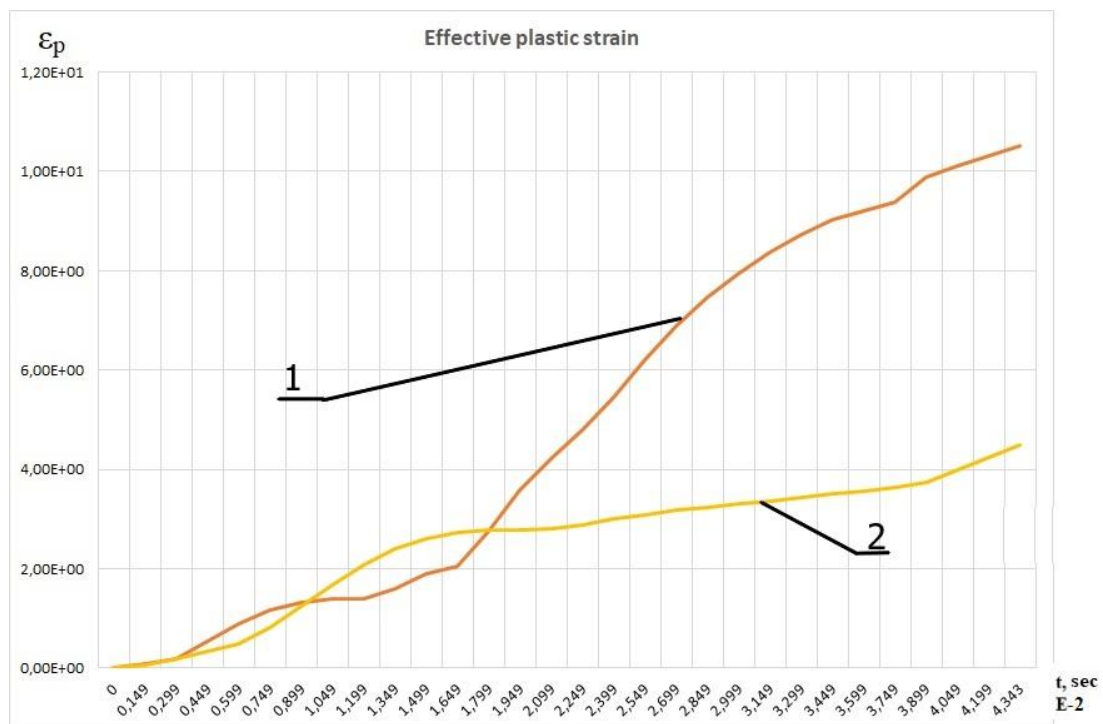


**Figure 6.** Change of effective plastic strain for nickel-chromium alloy of Inconel 718 grade and C45E steel according to simulation results

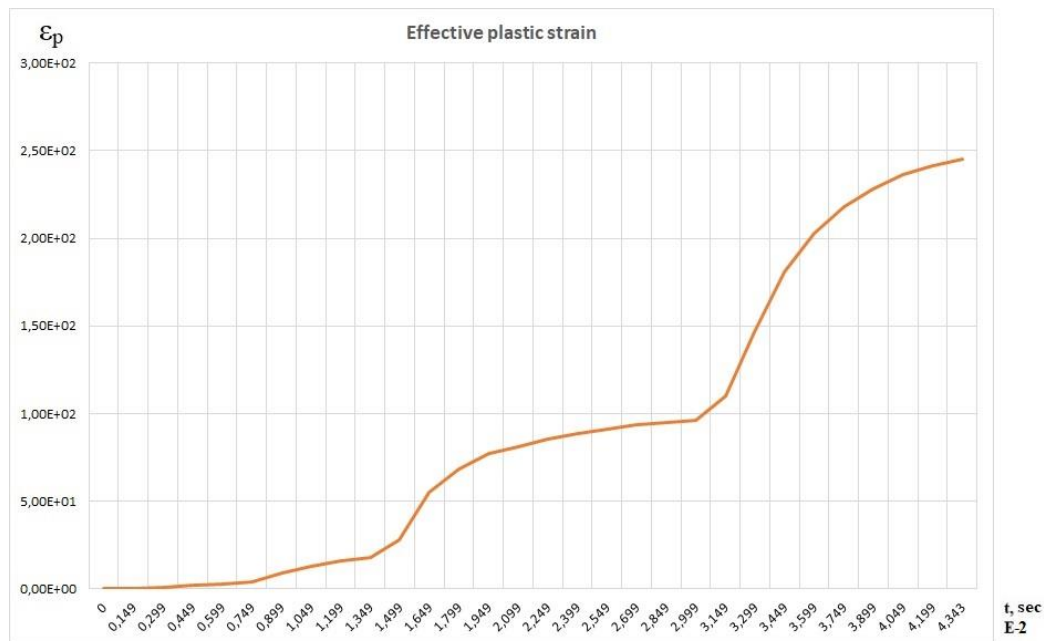


**Figure 7.** Change of effective plastic strain for A2024-T351 grade aluminum alloy according to the simulation results

As we can see from the graph of Fig. 7, one spindle revolution corresponds to one step of the sharp change in effective plastic deformation, which is caused by workpiece surface work-hardening on the previous tool revolution, as while cutting a new work-hardened layer of material there are modified plastic deformations. And the material becomes less susceptible to cutting, so when removing a new layer of workpiece material the required value of plastic deformation for material model fracture increases.

**Conclusions.** Due to the smoothed particle method, boring is simulated for three materials, such as heat-resistant Inconel 718 grade nickel-chromium alloy, C45E grade steel and A2024-T351 grade aluminum alloy. Graphs of cutting forces from modeling results are obtained. The obtained graphs of cutting forces are investigated. Equivalent stresses for the workpiece have peak when cutting the tool and gradually decrease during cutting. The change in the effective plastic deformation during modeling has a period corresponding to one workpiece revolution. This is caused by workpiece surface work-hardening on the previous tool revolution. According to the simulation results, the workpiece material influences the generation of regenerative fluctuations during boring and the magnitude of cutting forces.

## References

1. Eckart Uhlmann, Enrico Barth. Smoothed Particle Hydrodynamics simulation of the machining process of Inconel 718. *Procedia Manufacturing*. 2018. Vol. 18. P. 1–11.
2. Fabian Spreng, Peter Eberhard. Machining Process Simulations with Smoothed Particle Hydrodynamics. *Procedia CIRP*. 2015. P. 94–99.
3. Madaj M, Piska M. On the SPH Orthogonal Cutting Simulation of A2024-T351 Alloy. *Procedia CIRP*. 2013. Vol. 8. P. 152–157. DOI: <https://doi.org/10.1016/j.procir.2013.06.081>
4. On the selection of Johnson-Cook constitutive model parameters for Ti-6Al-4V using three types of numerical models of orthogonal cutting.
5. The influence of Johnson-Cook material constants on finite element simulation of machining of AISI 316L steel.
6. Impact of anisotropy and viscosity to model the mechanical behavior of Ti-6Al-4V alloy.
7. Uhlmann E, v. d. Schulenburg MG, Zettier R. Finite Element Modeling and Cutting Simulation of Inconel 718. *CIRP Annals* 2007;56:61–64. DOI: <https://doi.org/10.1016/j.cirp.2007.05.017>

8. P. W. Cleary, M. Prakash, R. Das, J. Ha. Modelling of Metal Forging Using SPH. *Applied Mathematical Modeling*. 2012. Vol. 36. Issue 8. P. 3836–3855. DOI: <https://doi.org/10.1016/j.apm.2011.11.019>
9. Balbaa M. A., Nasr Mohamed NA. Prediction of Residual Stresses after Laser-assisted Machining of Inconel 718 Using SPH. In: Schulze V, editor. *Proceedings of the 15th CIRP Conference on Modelling of Machining Operations*. Vol. 31. Amsterdam: Elsevier B. V.; 2015. P. 19–23. DOI: <https://doi.org/10.1016/j.procir.2015.03.034>
10. Heisel U., Zaloga W., Krivoruchko D., Storchak M., Goloborodko L. Modelling of orthogonal cutting processes with the method of smoothed particle hydrodynamics. *Production Engineering* 2013;7(6):639-645. DOI: <https://doi.org/10.1007/s11740-013-0484-0>
11. Feng Zhang, Zheng Liu, Yue Wang, Pingli Mao, Xinwen Kuang, Zhenglai Zhang, Yingdong Ju, Xiaozhong Xu, The modified temperature term on Johnson-Cook constitutive model of AZ31 magnesium alloy with {0002} texture. *Journal of Magnesium and Alloys*. Vol. 8. Issue 1. 2020. P. 172–183. ISSN 2213-9567. DOI: <https://doi.org/10.1016/j.jma.2019.05.013>
12. Spreng F., Schnabel D., Mueller A., Eberhard P., 2014. A local adaptive discretization algorithm for Smoothed Particle Hydrodynamics, *Computational Particle Mechanics*, 1 (2) : 131–145. DOI: <https://doi.org/10.1007/s40571-014-0015-6>
13. Xi Y, Bermingham M, Wang G, Dargusch M. SPH/FE modeling of cutting force and chip formation during thermally assisted machining of Ti6Al4V alloy. *Computational Materials Science* 2014;84:188-197. DOI: <https://doi.org/10.1016/j.commatsci.2013.12.018>
14. Livermore Software Technology Corporation (LSTC), 2012, *LSDYNA: Keyword User's Manual – Volume II: Material Models*, California.
15. Gaugele T., Eberhard P., 2013. Simulation of cutting processes using meshfree Lagrangian particle methods, *Computational Mechanics*, 51(3):261–278. DOI: <https://doi.org/10.1007/s00466-012-0720-z>
16. H. Li and E. Du, “Simulation of rock fragmentation induced by a tunnel boring machine disk cutter”, *Advances in Mechanical Engineering*. Vol. 8. No. 6. P. 1–11. 2016. DOI: <https://doi.org/10.1177/1687814016651557>
17. D. Parle, R. Singh and S. Joshi, “Modeling of Specific Cutting Energy in Micro-Cutting using SPH Simulation”, *IWMF2014, 9th INTERNATIONAL WORKSHOP ON MICROFACTORIES*. P. 121–126. 2014.
18. N. Chandiramani and T. Pothala, “Dynamics of 2-dof regenerative chatter during turning”. *Journal of Sound and Vibration*. Vol. 290. No. 1–2. P. 448–464. 2006. DOI: <https://doi.org/10.1016/j.jsv.2005.04.012>

#### Список використаної літератури

1. Eckart Uhlmann, Enrico Barth. Smoothed Particle Hydrodynamics simulation of the machining process of Inconel 718. *Procedia Manufacturing*. 2018. Vol. 18. P. 1–11.
2. Fabian Spreng, Peter Eberhard. Machining Process Simulations with Smoothed Particle Hydrodynamics. *Procedia CIRP*. 2015. P. 94–99.
3. Madaj M, Piska M. On the SPH Orthogonal Cutting Simulation of A2024-T351 Alloy. *Procedia CIRP*. 2013. Vol. 8. P. 152–157. DOI: <https://doi.org/10.1016/j.procir.2013.06.081>
4. On the selection of Johnson-Cook constitutive model parameters for Ti-6Al-4V using three types of numerical models of orthogonal cutting.
5. The influence of Johnson–Cook material constants on finite element simulation of machining of AISI 316L steel.
6. Impact of anisotropy and viscosity to model the mechanical behavior of Ti–6Al–4V alloy.
7. Uhlmann E, v. d. Schulenburg MG, Zettier R. Finite Element Modeling and Cutting Simulation of Inconel 718. *CIRP Annals* 2007;56:61–64. DOI: <https://doi.org/10.1016/j.cirp.2007.05.017>
8. P. W. Cleary, M. Prakash, R. Das, J. Ha. Modelling of Metal Forging Using SPH. *Applied Mathematical Modeling*. 2012. Vol. 36. Issue 8. P. 3836–3855. DOI: <https://doi.org/10.1016/j.apm.2011.11.019>
9. Balbaa M. A., Nasr Mohamed NA. Prediction of Residual Stresses after Laser-assisted Machining of Inconel 718 Using SPH. In: Schulze V, editor. *Proceedings of the 15th CIRP Conference on Modelling of Machining Operations*. Vol. 31. Amsterdam: Elsevier B. V.; 2015. P. 19–23. DOI: <https://doi.org/10.1016/j.procir.2015.03.034>
10. Heisel U., Zaloga W., Krivoruchko D., Storchak M., Goloborodko L. Modelling of orthogonal cutting processes with the method of smoothed particle hydrodynamics. *Production Engineering* 2013;7(6):639-645. DOI: <https://doi.org/10.1007/s11740-013-0484-0>
11. Feng Zhang, Zheng Liu, Yue Wang, Pingli Mao, Xinwen Kuang, Zhenglai Zhang, Yingdong Ju, Xiaozhong Xu, The modified temperature term on Johnson-Cook constitutive model of AZ31 magnesium alloy with {0002} texture. *Journal of Magnesium and Alloys*. Vol. 8. Issue 1. 2020. P. 172–183. ISSN 2213-9567. DOI: <https://doi.org/10.1016/j.jma.2019.05.013>
12. Spreng F., Schnabel D., Mueller A., Eberhard P., 2014. A local adaptive discretization algorithm for Smoothed Particle Hydrodynamics, *Computational Particle Mechanics*, 1 (2): 131–145. DOI: <https://doi.org/10.1007/s40571-014-0015-6>

13. Xi Y, Bermingham M, Wang G, Dargusch M. SPH/FE modeling of cutting force and chip formation during thermally assisted machining of Ti6Al4V alloy. Computational Materials Science 2014;84:188-197. DOI: <https://doi.org/10.1016/j.commatsci.2013.12.018>
14. Livermore Software Technology Corporation (LSTC), 2012, LSDYNA: Keyword User's Manual – Volume II: Material Models, California.
15. Gaugele T., Eberhard P., 2013. Simulation of cutting processes using meshfree Lagrangian particle methods, Computational Mechanics, 51(3):261–278. DOI: <https://doi.org/10.1007/s00466-012-0720-z>
16. H. Li and E. Du, «Simulation of rock fragmentation induced by a tunnel boring machine disk cutter», Advances in Mechanical Engineering. Vol. 8. No. 6. P. 1–11. 2016. DOI: <https://doi.org/10.1177/1687814016651557>
17. D. Parle, R. Singh and S. Joshi, «Modeling of Specific Cutting Energy in Micro-Cutting using SPH Simulation», IWMF2014, 9th INTERNATIONAL WORKSHOP ON MICROFACTORIES. P. 121–126. 2014.
18. N. Chandiramani and T. Pothala, «Dynamics of 2-dof regenerative chatter during turning». Journal of Sound and Vibration. Vol. 290. No. 1–2. P. 448–464. 2006. DOI: <https://doi.org/10.1016/j.jsv.2005.04.012>

## УДК 621.7

# МОДЕЛЮВАННЯ РОЗТОЧУВАННЯ МЕТОДОМ ЗГЛАДЖЕНИХ ЧАСТОК ГІДРОДИНАМІКИ

**Максим Шихалєєв**

*Національний технічний університет України «Київський політехнічний інститут імені Ігоря Сікорського», Київ, Україна*

**Резюме.** Розглянуто можливість застосування методу згладжених часток гідродинаміки для моделювання процесів оброблення різанням на прикладі багатолезового розточування отворів. Метод згладжених частинок гідродинаміки все ширше використовується вченими при розробленні комп'ютерних моделей оброблення різанням. В якості програмного пакета для моделювання використано високо-нелінійний вирішувач LS-Dyna з явною постановкою задачі динамічного моделювання (Explicit dynamics). В якості моделі матеріалу заготовки використано формулювання за Джонсоном-Куком (Johnson-Cook) з відповідними емпіричними коефіцієнтами для кожного матеріалу. Також наведено механічні характеристики матеріалу, потрібні для моделювання у вирішувачі LS-Dyna. Для матеріалу заготовки змінювався матеріал, а режими різання залишались однаковими для всіх матеріалів відповідно. Заготовку згенеровано за допомогою методу згладжених частинок, а інструмент – сіткою. Для спрощення моделі використано абсолютно твердий інструмент (Rigid). Кінематичну схему обертання інструменту реалізовано за допомогою ключового слова INITIAL\_VELOCITY\_GENERATION. Для надання поступального руху інструменту та закріплення заготовки використано ключове слово BOUNDARY\_PRESCRIBED\_MOTION вирішувача. Для моделювання використано один комп'ютер з двоядерним процесором і частотою 3.3 МГц. Найбільший крок інтегрування для збіжності при чисельному розв'язуванні задачі оброблення лімітовано критерієм Куранта-Фрідрікса-Леві. Отримані в програмному пакеті результати моделювання показано у вигляді графіків, які побудовано з використанням внутрішніх інструментів та інтерпретатора вирішувача LS-Dyna. Як бачимо, коливання сил різання при однакових режимах різання для різних матеріалів різні, а ефективна пластична деформація зростає пропорційно. Коливання сили різання при розточуванні в заданій моделі має найбільшу амплітуду для алюмінієвого сплаву марки A2024-T351. Для решти двох матеріалів коливання сил різання мають меншу амплітуду і пікове значення сили різання. Відповідно, найменше коливання сил різання отримано для сталі марки C45E. Зміни еквівалентних напружень за Мізесом теж змінюються за складним законом, але мають пікове значення при врізуванні різального інструменту.

**Ключові слова:** розточування, динаміка різання, метод згладжених часток гідродинаміки, безсітковий метод моделювання, FEM, SPH, моделювання оброблення.

[https://doi.org/10.33108/visnyk\\_tntu2021.03.013](https://doi.org/10.33108/visnyk_tntu2021.03.013)

Отримано 01.09.2020